iJRASET
International Journal For Research in Applied Science and Engineering Technology

INTERNATIONAL JOURNAL FOR RESEARCH

IN APPLIED SCIENCE & ENGINEERING TECHNOLOGY

Volume: 14 **Issue:** IX **Month of publication:** September 2026

DOI: https://doi.org/10.22214/ijraset.2026.84960

www.ijraset.com

Call: 08813907089 | E-mail ID: ijraset@gmail.com

International Journal for Research in Applied Science & Engineering Technology (IJRASET)
ISSN: 2321-9653; IC Value: 45.98; SJ Impact Factor: 7.538
Volume 14 Issue IX Sep 2026- Available at www.ijraset.com

Dam Break Analysis and Flood Inundation Mapping of Polavaram Dam Using HEC-RAS

Thota Tejaswi[1], Dr. Vemu Sreenivasulu[2]
[1]*Post Graduate Student, JNTUK, Kakinada,* [2]*Professor Department of Civil Engineering, University College of Engineering Kakinada (A), JNTUK, Kakinada, Andhra Pradesh, India*

Abstract: ***Failure of a dam can release a large volume of stored water suddenly and endanger the population and property downstream. This study presents a two-dimensional dam break analysis and flood inundation mapping of the Polavaram Dam, a multipurpose project on the Godavari River in Eluru District, Andhra Pradesh, India, using HEC-RAS 6.6. The reservoir was represented by a storage area and the downstream floodplain by a 2-D flow area with a 50 m mesh, built on SRTM 30 m terrain data and Esri 10 m land use/land cover data. Breach of the earth-cum-rock-fill (ECRF) dam section was simulated for overtopping and piping failure using five empirical breach methods, namely Froehlich (2008), Froehlich (1995), Von Thun and Gillette, Xu and Zhang, and MacDonald et al., for a simulation period of 24 hours. The Froehlich (2008) overtopping scenario gave the highest peak breach discharge of 174,862 m³/s and the largest inundation area of 717.224 km²; the corresponding piping scenario gave 120,453 m³/s and 559.097 km². Across the ten scenarios the inundation area ranged from 172.863 km² to 717.224 km². Maximum flood depth, velocity and water surface elevation were extracted at three downstream locations, where the maximum depth reached 17.138 m at Area 1. The results show that the choice of breach method strongly affects the peak discharge and flood extent, and the maps and values obtained can support emergency action planning and flood-hazard assessment downstream of the dam.***

Keywords: Dam break analysis, Polavaram Dam, HEC-RAS, flood inundation mapping, breach parameters, overtopping, piping, 2-D hydrodynamic modelling.

I. INTRODUCTION

Dams store water for irrigation, hydropower, water supply and flood moderation, but the same stored water becomes a serious hazard if a dam fails. A sudden breach releases a flood wave that can travel a long distance downstream with high depth and velocity, threatening lives, infrastructure and agriculture [6]. Dam break analysis is therefore carried out to estimate the breach outflow, the depth and velocity of the flood wave and the extent of inundation, which form the basis of emergency action plans.

Embankment dams, including earth-cum-rock-fill (ECRF) dams, fail mainly by overtopping and by piping, that is, internal erosion [1], [2]. The size of the breach and the rate at which it develops control the outflow hydrograph. These are usually estimated with empirical equations developed from case histories of past dam failures, and different equations can give different breach dimensions and peak discharges for the same dam [1]–[5]. HEC-RAS is widely used for dam break analysis and flood inundation mapping. Xiong [7] described a dam break analysis using HEC-RAS, and it has since been applied to dams in Iran [19], Ethiopia [20], Malaysia [21] and Uganda [22]. Two-dimensional HEC-RAS can simulate the spreading of a dam break flood wave over natural terrain using digital elevation and land use data [23], and several studies combined HEC-RAS with HEC-GeoRAS [24] to prepare the geometry [20], [22]. A more detailed review of these and other related studies is given in Section III.

The Polavaram Dam on the Godavari River is a large multipurpose project with a gross storage of 194.604 TMC at full reservoir level and a catchment area of 306,643 km². A failure of this dam would release a large volume of water into the downstream Godavari valley, and the objectives and scope of the present study are set out below.

II. OBJECTIVES OF THE STUDY

The main objectives of the present study are:

1) To perform two-dimensional dam break analysis of Polavaram Dam using HEC-RAS.
2) To simulate piping and overtopping failure scenarios.
3) To estimate breach parameters and generate breach flood hydrographs using different empirical methods.
4) To determine the peak discharge resulting from different breach scenarios.
5) To generate flood inundation maps for the downstream area.

©IJRASET: All Rights are Reserved

6) To determine important hydraulic parameters such as water depth, water surface elevation, and flow velocity.
7) To compare the results obtained from different empirical breach methods for piping and overtopping conditions.

III. LITERATURE REVIEW

A number of studies have applied HEC-RAS to dam break analysis and flood inundation mapping worldwide. Xiong [7] demonstrated an early one-dimensional dam break analysis using HEC-RAS. Two-dimensional HEC-RAS has since been used to simulate hypothetical or historical dam failures in many settings: Khosravi et al. [19] mapped the flood from a hypothetical failure of the Sefid-Roud Dam, Iran; Leoul and Kassahun [20] analysed the Kesem Kebena Dam, Ethiopia, combining HEC-RAS with HEC-GeoRAS; Shahrim and Ros [21] studied the Temenggor Dam, Malaysia, comparing 1-D and 2-D breach hydrographs; and Kiwanuka et al. [22] examined the Kibimba Dam, Uganda, again using HEC-RAS with HEC-GeoRAS.

Several recent studies have focused on the sensitivity of dam break results to the breach method and the model set-up. Karim et al. [8] used 2-D HEC-RAS to model the overtopping failure of the Al-Udhaim Dam, Iraq, and the propagation of the flood wave 100 km downstream. Hosseinzadeh-Tabrizi et al. [9] simulated dam-breach flood waves and compared the resulting hydrographs against analytical solutions. Mo et al. [10] used a 1-D HEC-RAS model to study dam-break flood routing for full, half and one-third breach widths of an earth-rock dam, and found that a 1 m rise in the bursting water level increased the peak flow by about 7% and delayed the peak by around 1.5 hours. Paşa et al. [11] simulated the potential failure of two consecutive dams, a concrete buttress dam followed by an earth-fill gravity dam. Mohamed et al. [12] modelled flood wave propagation from a piping failure using coupled 1-D/2-D HEC-RAS and reported that a finer terrain resolution gave clearer water depth and inundation results.

Other studies have examined the sensitivity of breach parameters and compared multiple empirical methods, which is also the approach taken in the present study. Basheer et al. [13] compared five breach-parameter prediction approaches and their influence on the flood hydrograph for the Mosul Dam, Iraq. Bhandari et al. [14] applied 2-D unsteady flow routing to map flood inundation for the lower Brazos River watershed, Texas. Balogun and Ganiyu [15] analysed a hypothetical failure of the Asa Dam, Nigeria, with HEC-RAS and HEC-GeoRAS. Yakti et al. [16] modelled the 2013 failure of the Way Ela natural landslide dam, Indonesia. Mhmood et al. [17] simulated the hypothetical overtopping failure of the Haditha Dam on the Euphrates River, Iraq, and reported the flood wave attenuation and inundation width along the study reach. Raman and Liu [18] used HEC-RAS with SRTM terrain data to reproduce the extent of the 2019 Brumadinho tailings dam failure, Brazil.

Taken together, these studies show that HEC-RAS is a well-established tool for dam break analysis, but also that the peak discharge, breach hydrograph and inundation extent obtained are sensitive to the breach method, the failure mode and the terrain resolution used. Few studies have compared as many as five empirical breach methods for both overtopping and piping failure on the same dam, which is the gap addressed in the present study of the Polavaram Dam.

IV. STUDY AREA

The Indira Sagar Polavaram Project is a multipurpose terminal project on the Godavari River, located about 42 km upstream of the Sir Arthur Cotton Barrage at Dowlaiswaram, near Ramayyapeta Village in Polavaram Mandal of Eluru District, Andhra Pradesh, India. The dam site is at 17°16′53″ N latitude and 81°39′46″ E longitude. Fig. 1 shows the location of the study area.

The project is a composite dam consisting of a concrete spillway and ECRF dam sections. The spillway is 1128.4 m long with 48 gates of 16 m × 20 m, and the ECRF dam is 2454 m long (564 m + 1750 m + 140 m, including Gaps 1, 2 and 3). The maximum height is 48.32 m for the non-overflow ECRF section and 63.25 m for the spillway section. The salient features of the project are given in Table I.

TABLE I
SALIENT FEATURES OF THE POLAVARAM PROJECT

Feature	Value	Feature	Value
Catchment area	306,643 km²	Spread area at FRL	552.4 km²
Location	17°16′53″ N, 81°39′46″ E	Length of spillway	1128.4 m
MWL = FRL	+45.72 m	Overflow / non-overflow section	768.0 m / 360.4 m
DSL = MDDL	+41.15 m	Spillway gates (16 m × 20 m)	48 Nos.
Spillway crest level	+25.72 m	Length of ECRF dam (incl. Gaps 1, 2, 3)	2454 m
TBL (ECRF)	+53.32 m	Deepest riverbed level	+8.24 m
Gross storage at FRL and MWL	194.604 TMC	Max. height, non-overflow (ECRF) dam	48.32 m
Storage at DSL	119.403 TMC	Max. height, spillway dam	63.25 m
Live storage	75.2 TMC	Max. flood discharge (design)	141,368.5 m³/s

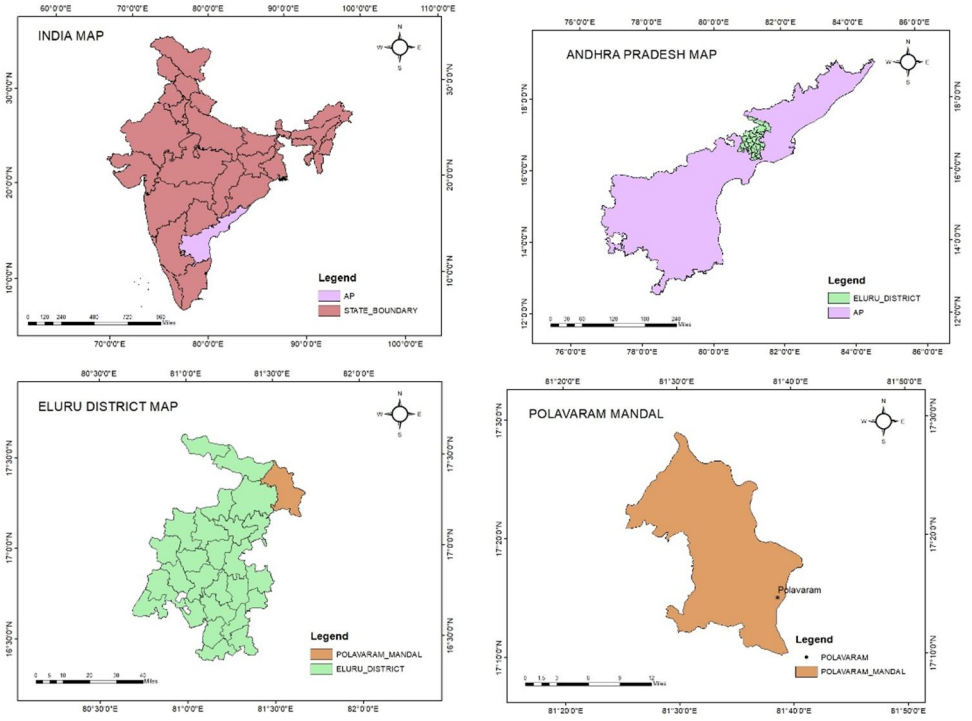

Fig. 1 Location of the study area: (a) India, (b) Andhra Pradesh, (c) Eluru District, and (d) Polavaram Mandal with the location of Polavaram.

V. DATA COLLECTION

A. Digital Elevation Model (DEM)

The terrain of the study area was represented by the SRTM digital elevation model (DEM) at 30 m resolution [25], [26] (Fig. 2a); the elevations in the study extent range from −21 m to 784 m. The DEM was imported into RAS Mapper as the terrain for the riverbed, the floodplain and the area downstream of the dam.

B. Land Use and Land Cover (LULC)

Land use and land cover were taken from the 2025 Esri 10 m global land use/land cover product, produced by Impact Observatory for Esri from Sentinel-2 imagery (Fig. 2b). The study area contains seven classes: water, trees, flooded Manning's roughness is an uncertain input of 2-D flood models [27], and appropriate values for each land cover class are needed to build an accurate model [28]. The Manning's n values in Table II are the values recommended for the Esri LULC classes in [28] and were assigned to the LULC layer so that every cell of the 2-D flow area carries a Manning's n

TABLE II
MANNING'S N VALUES FOR LULC CLASSES

LULC class	Manning's n
Water	0.038
Trees	0.126
Flooded vegetation	0.061
Crops	0.035
Built-up area	0.092
Bare ground	0.027
Range land	0.038

C. Reservoir Elevation–Area Curve

The reservoir was represented in HEC-RAS by a storage area. The relationship between the reservoir elevation and area (Fig. 3) was obtained from the Water Resources Department, Polavaram Irrigation Project Headwork Circle, and was used as the input data that defines the storage area.

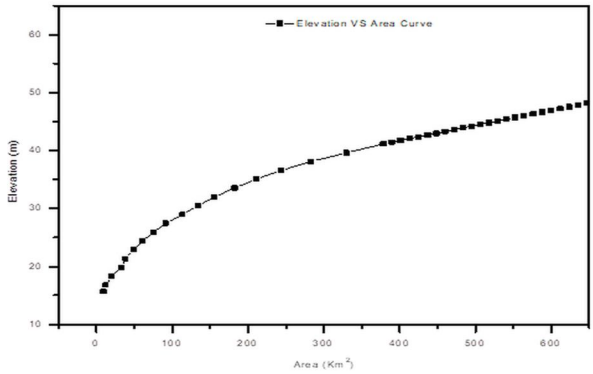

Fig. 3 Elevation–area curve of the Polavaram reservoir used as input for the storage area in HEC-RAS (data from the Water Resources Department, Polavaram Irrigation Project Headwork Circle).

D. Lateral Inflow Hydrograph

The inflow to the reservoir was applied as a lateral inflow hydrograph for 16 July 2022 (Fig. 4), also obtained from the Water Resources Department, Polavaram Irrigation Project Headwork Circle. The hydrograph rises from 1207.4 m³/s at hour 1 to a peak of 57,230.9 m³/s at hour 11 and then recedes to 13,848.5 m³/s at hour 24.

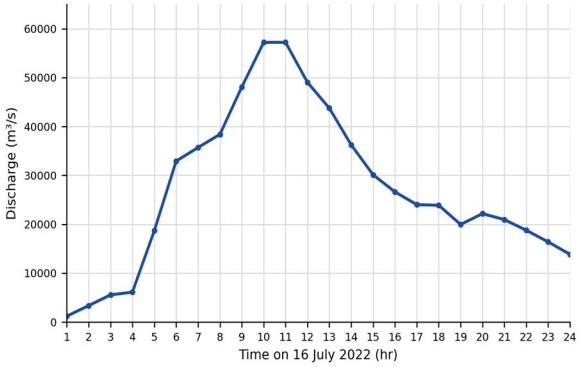

Fig. 4 Lateral inflow hydrograph of the Polavaram Dam for 16 July 2022 (data from the Water Resources Department, Polavaram Irrigation Project Headwork Circle).

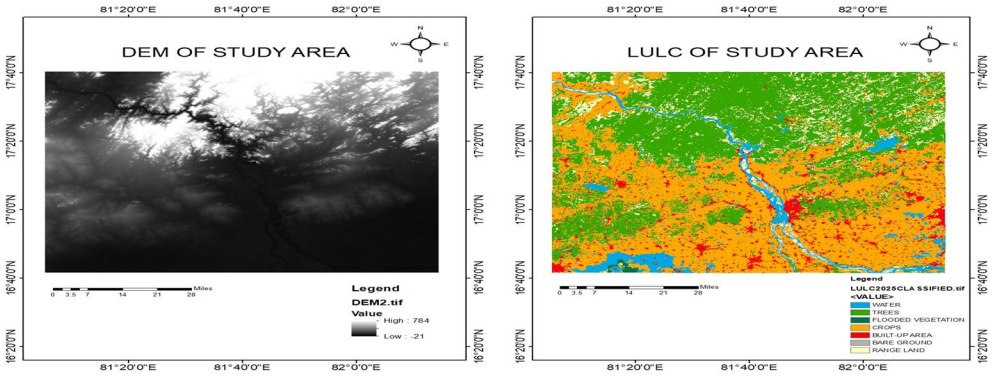

(a) (b)

Fig. 2 Data used in the study: (a) SRTM 30 m digital elevation model (elevation in m) and (b) Esri land use and land cover of the study area.

©IJRASET: All Rights are Reserved

ISSN: 2321-9653; IC Value: 45.98; SJ Impact Factor: 7.538
Volume 14 Issue IX Sep 2026- Available at www.ijraset.com

VI. METHODOLOGY

A. Model Setup

The dam break flood was simulated with HEC-RAS version 6.6 using 2-D unsteady flow [23]. The downstream floodplain was represented by a 2-D flow area, in which a computational mesh of 50 m × 50 m cell size was generated, with the surface roughness of each cell assigned from the LULC layer using the Manning's n values in Table II. The ECRF dam was drawn as an SA/2D connection between the storage area and the 2-D flow area, and the breach data were entered in this connection.

The lateral inflow hydrograph of Fig. 4 was applied as the inflow to the reservoir, and normal-depth boundary conditions, with an assigned friction slope of 0.8, were applied at the two downstream outlets, Outlet 1 and Outlet 2. The initial reservoir level was set through the storage area's elevation–area relationship (Fig. 3) together with the lateral inflow hydrograph of Fig. 4. Reference points were placed along the downstream river area, at A1, A2 and A3, to obtain the velocity, depth and water surface elevation of the flood wave. The simulation duration was 24 hours, matching the duration of the lateral inflow hydrograph. Fig. 5 shows the methodology followed in the study.

B. Breach Modelling

Only the ECRF dam section was considered to breach; the concrete spillway was not considered to fail. Two failure modes, piping and overtopping, were analysed. A piping failure starts when seepage through the dam erodes material and forms an opening that begins as a circular hole in the dam face. Flow through the circular opening is modelled as orifice flow [23],

$$Q = CA\sqrt{2gH} \quad (1)$$

where Q is the discharge, C is the orifice (piping) coefficient, A is the cross-sectional area of the orifice normal to the flow, g is the gravitational acceleration and H is the total energy head measured from the centre line of the orifice. When the opening reaches the top of the dam it expands as a trapezoid and the flow is modelled as weir flow. An overtopping failure starts when water flowing over the dam erodes the dam face; the breach begins at a point on the top of the dam and expands in a trapezoidal shape to its maximum size, defined by the top and bottom elevations, the bottom width and the side slopes. Flow through the expanding breach is modelled with the weir equation [23],

$$Q = C_1 bH^{1.5} + C_2 mH^{2.5} \quad (2)$$

where Q is the discharge over the breach (m^3/s), $C_1 = 1.7$ and $C_2 = 1.35$ are the discharge coefficients for the rectangular and triangular portions of the trapezoid, b is the bottom width of the breach, m is the side slope (H:V) and H is the upstream energy head above the breach.

The breach parameters were estimated with five regression methods: Froehlich (2008) [2], Froehlich (1995) [1], Von Thun and Gillette [4], Xu and Zhang [5] and MacDonald and Langridge-Monopolis [3]. This gave ten breach scenarios in total. The parameters were entered in HEC-RAS with the User Entered Data option, which needs the breach location, failure mode, breach shape (bottom elevation, bottom width and side slopes), critical breach development time, trigger mechanism, and the weir and piping coefficients. Common geometric inputs were used for all five methods: a dam crest width of 15 m, an upstream face slope Z1 of 3(H):1(V) and a downstream face slope Z2 of 2.5(H):1(V), with the dam classified as "dam with corewall" for the Xu and Zhang and Von Thun and Gillette methods, "non-homogeneous or rockfill" for the MacDonald method, and a medium dam erodibility. Table III and Fig. 6 illustrate the resulting breach parameters and the corresponding HEC-RAS breach data dialog for the piping failure scenario, using the Froehlich (2008) method as an example.

1) *Froehlich (2008):* This method was developed from data of 74 embankment dam failures and gives the average breach width B_{ave} and the breach formation time t_f as

$$B_{ave} = 0.27 K_o V_w^{0.32} h_b^{0.04} \quad (3)$$

$$t_f = 63.2\sqrt{\frac{V_w}{gh_b^2}} \quad (4)$$

where K_o is 1.3 for overtopping and 1.0 for piping, V_w is the reservoir volume at the time of failure (m^3), h_b is the height of the final breach (m), g is the gravitational acceleration (9.80665 m/s^2) and t_f is in seconds. The average side slopes are 1.0H:1V for overtopping and 0.7H:1V for piping.

2) *Froehlich (1995):* This method was developed from data of 63 embankment dam failures:

$$B_{ave} = 0.1803 K_o V_w^{0.32} h_b^{0.19} \quad (5)$$

$$t_f = 0.00254 V_w^{0.53} h_b^{-0.90} \quad (6)$$

©IJRASET: All Rights are Reserved

where K_o is 1.4 for overtopping and 1.0 for piping and t_f is in hours. The average side slopes are 1.4H:1V for overtopping and 0.9H:1V for piping.

3) *Von Thun and Gillette (1990):* This method used 57 dams. The average breach width is

$$B_{ave} = 2.5h_w + C_b \quad (7)$$

where h_w is the depth of water above the bottom of the breach (m) and C_b depends on the reservoir size: 6.1 m for volumes below 1.23×10^6 m³, 18.3 m for 1.23×10^6 to 6.17×10^6 m³, 42.7 m for 6.17×10^6 to 1.23×10^7 m³, and 54.9 m above 1.23×10^7 m³. The breach side slopes are 1.0H:1.0V. The breach formation time t_f (hours) is given as a function of h_w for erosion-resistant (8) and easily erodible (9) dams,

$$t_f = 0.02h_w + 0.25 \quad (8)$$

$$t_f = 0.015h_w \quad (9)$$

and as a function of h_w and B_{ave} for erosion-resistant (10) and easily erodible (11) dams,

$$t_f = \frac{B_{ave}}{4h_w} \quad (10)$$

$$t_f = \frac{B_{ave}}{4h_w + 61.0} \quad (11)$$

4) *Xu and Zhang (2009):* This method is based on earth and rockfill dam failures. The average breach width B_{ave}, the breach top width B_t and the side slope Z are

$$\frac{B_{ave}}{h_b} = 0.787\left(\frac{h_d}{h_r}\right)^{0.133}\left(\frac{V_w^{1/3}}{h_w}\right)^{0.652} e^{B_3} \quad (12)$$

$$\frac{B_t}{h_b} = 1.062\left(\frac{h_d}{h_r}\right)^{0.092}\left(\frac{V_w^{1/3}}{h_w}\right)^{0.508} e^{B_2} \quad (13)$$

$$Z = \frac{B_t - B_{ave}}{h_b} \quad (14)$$

where h_d is the height of the dam (m), $h_r = 15$ m is a reference height that separates large and small dams, and B_2 and B_3 each equal $b_3 + b_4 + b_5$. For B_3, $b_3 = -0.041$, 0.026 and −0.226 for dams with corewalls, concrete-faced dams and homogeneous/zoned-fill dams; $b_4 = 0.149$ and −0.389 for overtopping and seepage/piping; and $b_5 = 0.291$, −0.14 and −0.391 for high, medium and low dam erodibility. For B_2, $b_3 = 0.061$, 0.088 and −0.089; $b_4 = 0.299$ and −0.239; and $b_5 = 0.411$, −0.062 and −0.289 for the same classes. The breach formation time is

$$\frac{T_f}{T_r} = 0.304\left(\frac{h_d}{h_r}\right)^{0.707}\left(\frac{V_w^{1/3}}{h_w}\right)^{1.228} e^{B_5} \quad (15)$$

where T_f is the formation time (hours), $T_r = 1$ hour, and $B_5 = b_3 + b_4 + b_5$ with $b_3 = -0.327$, −0.674 and −0.189; $b_4 = -0.579$ and −0.611; and $b_5 = -1.205$, −0.564 and 0.579 for the same classes. This equation usually gives longer formation times than the other methods and is not recommended for use in HEC-RAS, so it is given here for completeness; HEC-RAS computed a formation time of 35.83 hours from this equation for the piping scenario (Table III).

5) *MacDonald and Langridge-Monopolis (1984):* This method relates the volume of material eroded from the dam to the reservoir volume released and the head on the breach at failure [3]. The eroded volume is

$$V_e = C_v V_w^{0.769} h_w^{0.769} \quad (16)$$

where V_e is the volume of material eroded from the dam (m³), V_w is the volume of water released from the reservoir at breach failure (m³), h_w is the depth of water above the breach invert (m), and C_v is a coefficient equal to 0.0261 for earthfill dams and 0.00348 for non-earthfill (rockfill or non-homogeneous) dams; the ECRF dam of this study, classified as non-homogeneous/rockfill, used the latter value. The eroded volume is related to the breach geometry through the trapezoidal breach cross-section,

$$V_e = \frac{B_b + B_t}{2} h_b L \quad (17)$$

where B_b and B_t are the breach bottom and top width (m), h_b is the breach depth (m) and L is the effective length of the eroded dam section (m). The breach formation time is

$$t_f = 0.0179 V_e^{0.364} \quad (18)$$

with t_f in hours and V_e in m³ [3]. The ratio BEI = V_w/V_e, termed the breach erosion index, is sometimes used alongside these equations to relate the erodibility of the dam material to the observed case histories.

Fig. 6 shows the HEC-RAS breach data dialog for the piping failure scenario with the Froehlich (2008) method selected: a top of dam elevation of 48.77 m, a breach bottom elevation of 3.05 m at center station 600, a pool elevation at failure of 43.89 m and a pool volume at failure of 4.48 × 10^7 (in units of 1000 m³), giving a final bottom width of 774 m, side slopes of 0.7H:1V, a breach weir coefficient of 1.44, a piping coefficient of 0.5 and an initial piping elevation of 40 m, with the breach triggered at a reservoir water-surface elevation of 43.89 m.

.

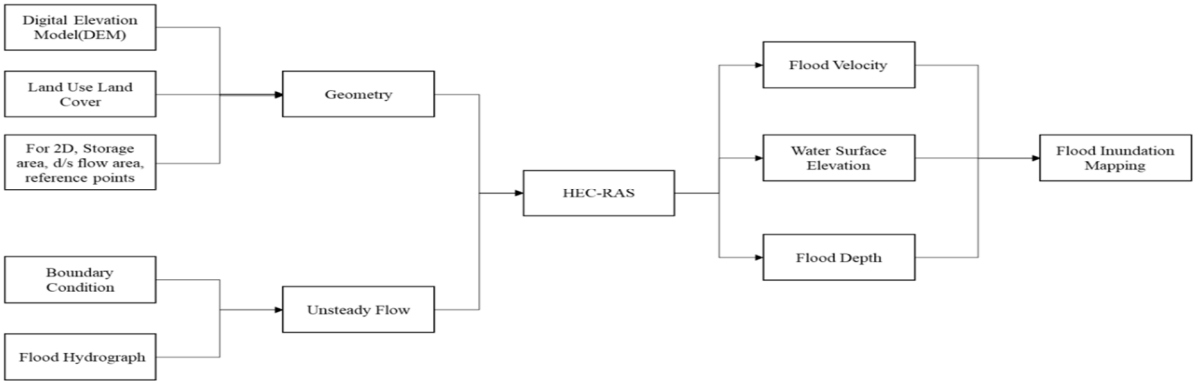

Fig.5 Methodology flow chart of the dam break analysis and flood inundation mapping.

TABLE III
BREACH PARAMETERS COMPUTED BY THE HEC-RAS PARAMETER CALCULATOR (PIPING FAILURE)

Method	Breach bottom width (m)	Side slopes (H:V)	Breach development time (hr)
MacDonald et al.	15141	0.5	14.48
Froehlich (1995)	913	0.9	35.97
Froehlich (2008)	774	0.7	25.95
Von Thun & Gillette	134	0.5	1.07
Xu & Zhang	459	−0.54	35.83

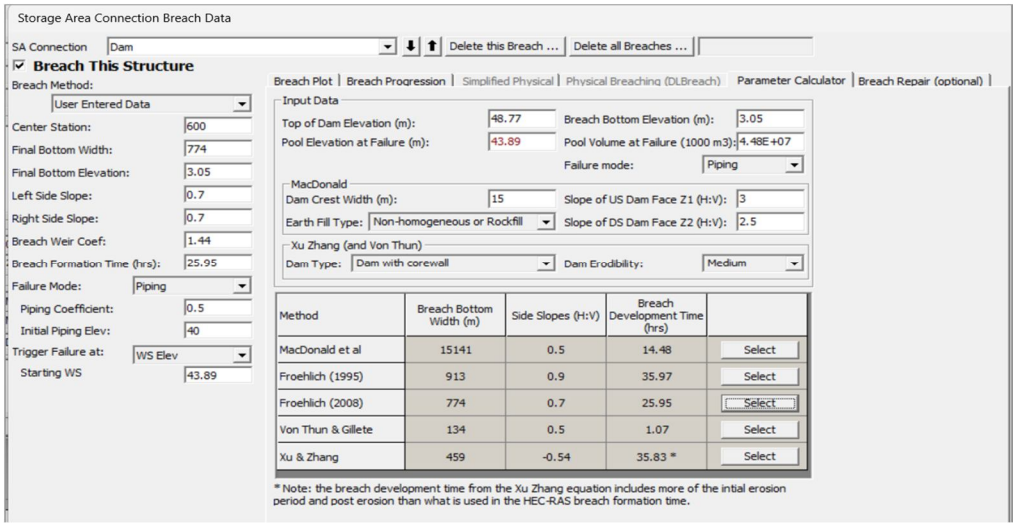

Fig. 6 HEC-RAS Storage Area Connection breach data dialog, showing the input for the piping failure scenario with the Froehlich (2008) method selected.

C. Flood Routing

HEC-RAS routes the flood wave produced by the breach over the 2-D flow area by solving the shallow water equations in diffusion wave form [23],

$$\frac{\partial \eta}{\partial t} = \nabla \cdot (\beta \nabla \eta) + q \qquad (19)$$

where η is the water surface elevation, t is time, q is a source/sink term and β is a diffusion coefficient computed from Manning's n, the flow depth and the water surface slope at each cell face [23]. This equation is solved together with continuity to give the depth, velocity and water surface elevation used to build the flood inundation maps in Section VII.

VII. RESULTS AND DISCUSSION

A. Breach Outflow and Inundation Area

Table IV gives the maximum breach width, the peak breach discharge and the inundation area for the ten scenarios. The Froehlich (2008) overtopping scenario produced the largest breach (maximum width 753.04 m), the highest peak discharge of 174,862 m³/s and the largest inundation area of 717.224 km². The corresponding piping scenario gave a maximum breach width of 580.78 m, a peak discharge of 120,453 m³/s and an inundation area of 559.097 km². The Froehlich (1995) method gave peak discharges of 171,516 m³/s for overtopping and 74,778 m³/s for piping, with inundation areas of 715.053 km² and 542.004 km².

TABLE IV
BREACH WIDTH, PEAK DISCHARGE AND INUNDATION AREA

Breach method	Failure mode	Max. breach width (m)	Peak discharge (m³/s)	Inundation area (km²)
Froehlich (2008)	Overtopping	753.04	174,862	717.224
	Piping	580.78	120,453	559.097
Froehlich (1995)	Overtopping	684.11	171,516	715.053
	Piping	490.67	74,778	542.004
Von Thun & Gillette	Overtopping	120.00	37,945	540.219
	Piping	120.00	37,954	538.369
Xu & Zhang	Overtopping	416.17	83,912	643.021
	Piping	250.57	32,434	172.863
MacDonald et al.	Overtopping	365.00	106,516	715.657
	Piping	365.00	106,786	700.102

With the Von Thun and Gillette method the maximum breach width was 120.00 m for both failure modes, and the peak discharges were almost the same, 37,945 m³/s for overtopping and 37,954 m³/s for piping, with inundation areas of 540.219 km² and 538.369 km². The Xu and Zhang method gave a peak discharge of 83,912 m³/s and an inundation area of 643.021 km² for overtopping, against 32,434 m³/s and 172.863 km² for piping. The MacDonald et al. method gave peak discharges of 106,516 m³/s and 106,786 m³/s and inundation areas of 715.657 km² and 700.102 km² for overtopping and piping respectively. For every method, overtopping produced a larger inundation area than piping. The difference was small for Von Thun and Gillette and for MacDonald et al., but large for Xu and Zhang, where the piping scenario kept the flood largely within the river corridor. The highest breach velocity ranged from 6.75 m/s (Froehlich 1995, piping) to 9.67 m/s (Xu and Zhang, overtopping). The peak discharge ranged from 32,434 m³/s (Xu and Zhang, piping) to 174,862 m³/s (Froehlich 2008, overtopping), a difference of more than five times, which shows how strongly the breach method controls the outflow.

B. Breach Flow Hydrographs

Fig. 7 compares the breach flow hydrographs of the five methods for overtopping and piping failure. In the overtopping scenarios (Fig. 7a), the Froehlich (2008) and Froehlich (1995) hydrographs rise steadily and were still increasing when the 24-hour simulation ended, reaching 174,862 m³/s and 171,516 m³/s. The MacDonald et al. hydrograph rises quickly to a peak of 106,516 m³/s at hour 5 and then recedes slowly to about 100,900 m³/s. The Von Thun and Gillette breach flow rises to about 37,945 m³/s by hour 2 and stays almost constant thereafter, and the Xu and Zhang breach flow increases unevenly, with a temporary drop to zero around hours 6–7, to a peak of 83,912 m³/s at hour 23.

©IJRASET: All Rights are Reserved | SJ Impact Factor 7.538 | ISRA Journal Impact Factor 7.894 |

In the piping scenarios (Fig. 7b), the Froehlich (2008) and Froehlich (1995) hydrographs again rise steadily to 120,453 m³/s and 74,778 m³/s and were still increasing at the end of the simulation. The MacDonald et al. hydrograph follows almost the same shape as in the overtopping case, peaking at 106,786 m³/s at hour 5 before receding to about 101,100 m³/s. The Von Thun and Gillette breach flow again levels off at about 37,954 m³/s from hour 2 onward, while the Xu and Zhang breach flow rises gradually to 32,434 m³/s by the end of the simulation, remaining well below the other four methods throughout. In both failure modes, the MacDonald et al. and Xu and Zhang (overtopping) hydrographs are the only ones that reach a clear peak and recede within the 24-hour window; the Froehlich (2008), Froehlich (1995) and Xu and Zhang (piping) hydrographs had not yet peaked when the simulation ended, so their true peak discharge may be higher than the 24-hour value reported in Table IV.

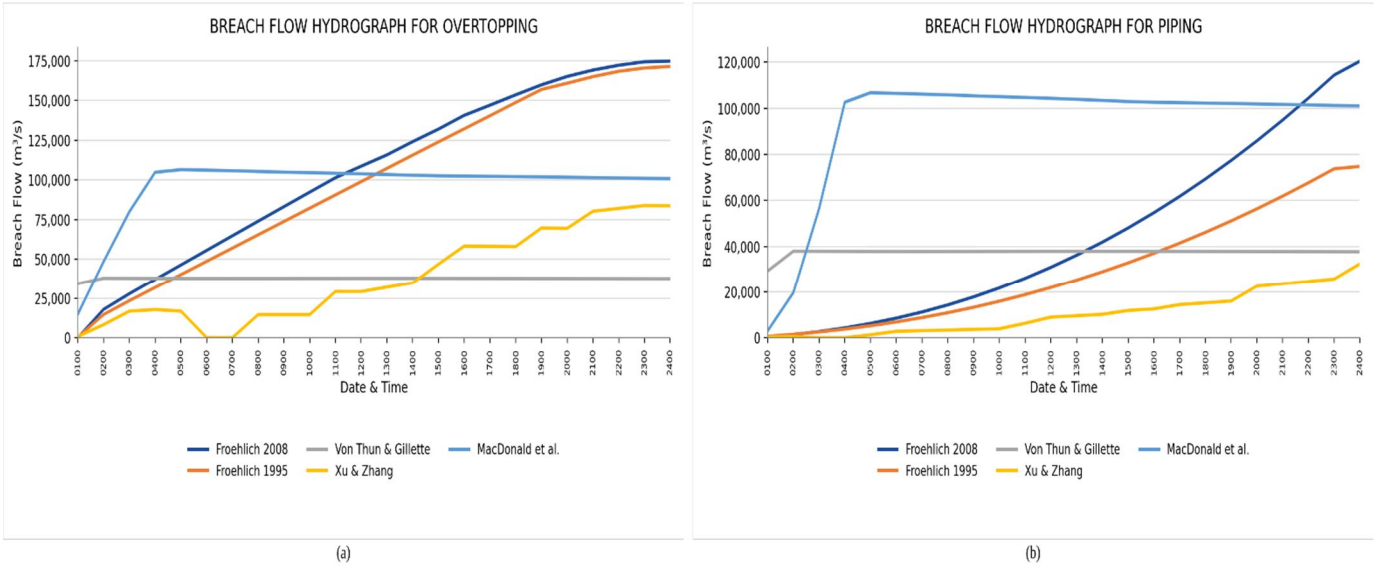

Fig. 7 Breach flow hydrographs of the five breach methods for (a) overtopping and (b) piping failure of the Polavaram Dam.

C. Flood Depth, Velocity and Water Surface Elevation

Tables V to VII give the maximum flood depth, flood-wave velocity and water surface elevation at Areas 1, 2 and 3 for the ten scenarios.

TABLE V
MAXIMUM FLOOD DEPTH (M) AT THE DOWNSTREAM AREAS

Breach method	Overtopping			Piping		
	Area 1	Area 2	Area 3	Area 1	Area 2	Area 3
Froehlich (2008)	14.071	8.288	15.772	13.945	3.492	5.790
Froehlich (1995)	16.651	8.403	13.813	9.073	2.467	5.195
Von Thun & Gillette	7.932	2.187	5.900	6.424	1.054	6.314
Xu & Zhang	17.138	2.551	9.816	11.384	0.317	3.020
MacDonald et al.	15.901	10.682	13.346	14.627	9.759	10.880

TABLE VI
MAXIMUM FLOOD-WAVE VELOCITY (M/S) AT THE DOWNSTREAM AREAS

Breach method	Overtopping			Piping		
	Area 1	Area 2	Area 3	Area 1	Area 2	Area 3
Froehlich (2008)	3.720	0.447	0.570	3.208	0.174	0.663
Froehlich (1995)	3.937	0.409	0.605	2.286	0.084	0.530
Von Thun & Gillette	2.816	0.088	0.738	3.366	0.312	0.528
Xu & Zhang	3.603	0.397	0.643	1.865	0.301	0.460
MacDonald et al.	3.524	0.308	0.566	3.858	0.378	0.775

TABLE VII
MAXIMUM WATER SURFACE ELEVATION (M) AT THE DOWNSTREAM AREAS

Breach method	Overtopping			Piping		
	Area 1	Area 2	Area 3	Area 1	Area 2	Area 3
Froehlich (2008)	36.455	34.160	33.932	32.449	27.185	24.783
Froehlich (1995)	35.826	32.955	32.597	30.320	25.972	23.764
Von Thun & Gillette	28.242	25.788	25.223	28.257	25.774	25.193
Xu & Zhang	32.681	28.454	27.535	27.874	24.375	20.851
MacDonald et al.	33.855	32.472	32.343	33.672	32.153	32.022

Area 1 experienced the highest flood-wave velocities in all scenarios, from 1.865 m/s to 3.937 m/s, compared with 0.084 m/s to 0.447 m/s at Area 2 and 0.460 m/s to 0.775 m/s at Area 3. The maximum flood depth was 17.138 m at Area 1 (Xu and Zhang, overtopping), 10.682 m at Area 2 (MacDonald et al., overtopping) and 15.772 m at Area 3 (Froehlich 2008, overtopping). The maximum water surface elevation was 36.455 m at Area 1, 34.160 m at Area 2 and 33.932 m at Area 3, all for the Froehlich (2008) overtopping scenario.

Overtopping gave a higher flood depth than piping in all cases except Von Thun and Gillette at Area 3, where piping gave the higher depth (6.314 m against 5.900 m). Overtopping also gave the higher water surface elevation for every method except Von Thun and Gillette, for which the two failure modes differed by less than 0.03 m. The maximum velocity at Area 3 was 0.775 m/s for piping (MacDonald et al.), slightly higher than the 0.738 m/s obtained for overtopping (Von Thun and Gillette).

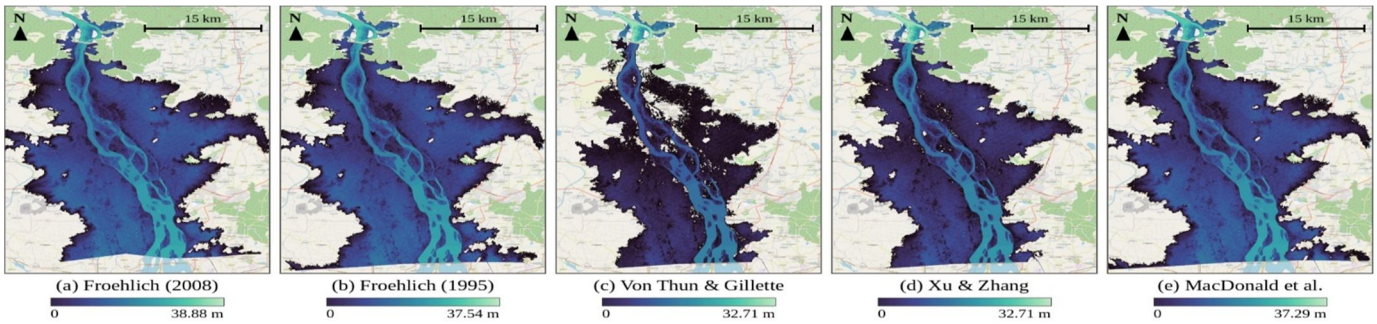

Fig. 8 Maximum flood depth maps for overtopping failure: (a) Froehlich (2008), (b) Froehlich (1995), (c) Von Thun & Gillette, (d) Xu & Zhang, and (e) MacDonald et al. The colour scale runs from 0 to the maximum depth given below each panel.

©IJRASET: All Rights are Reserved | SJ Impact Factor 7.538 | ISRA Journal Impact Factor 7.894 |

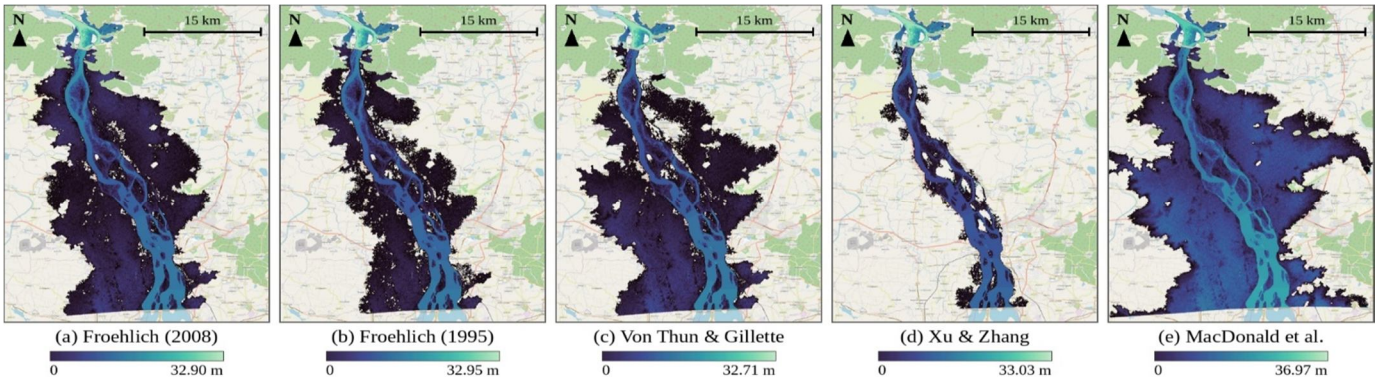

Fig. 9 Maximum flood depth maps for piping failure: (a) Froehlich (2008), (b) Froehlich (1995), (c) Von Thun & Gillette, (d) Xu & Zhang, and (e) MacDonald et al. The colour scale runs from 0 to the maximum depth given below each panel.

D. Flood Inundation Maps

Figs. 8 and 9 show the maximum flood depth maps for overtopping and piping failure respectively. The largest depths in the domain were 38.88 m and 32.90 m for Froehlich (2008), 37.54 m and 32.95 m for Froehlich (1995), 32.71 m for both modes for Von Thun and Gillette, 32.71 m and 33.03 m for Xu and Zhang, and 37.29 m and 36.97 m for MacDonald et al. (overtopping and piping respectively). The greatest depths occur in the main river channel and in the reach just downstream of the dam, while the floodplain on both banks is inundated to smaller depths. In all scenarios the flood wave reaches the downstream limit of the 2-D flow area.

The overtopping scenarios spread the flood widely over the floodplain on both sides of the river, whereas in the Xu and Zhang piping scenario the flood stays mainly along the river corridor, as reflected in its inundation area of 172.863 km². Fig. 10 shows the villages and towns that lie within the flood inundation boundary; the red line marks the extent of inundation obtained from the model, and numerous villages and small towns along the Godavari valley, including Polavaram itself, fall within it.

E. Influence of the Breach Method

The results show that, for the same dam and failure mode, the breach flow hydrograph, peak discharge, inundation area and depths at the downstream areas depend strongly on the empirical method used to define the breach. The Froehlich (2008) overtopping scenario gave the most severe condition in this study, while the Von Thun and Gillette and Xu and Zhang (piping) methods gave the least severe. Because the ten scenarios differ so much, a single method or a single downstream location is not enough to describe the flood hazard, and reporting a range of outcomes from several empirical methods, as done here, gives a more complete picture for emergency planning.

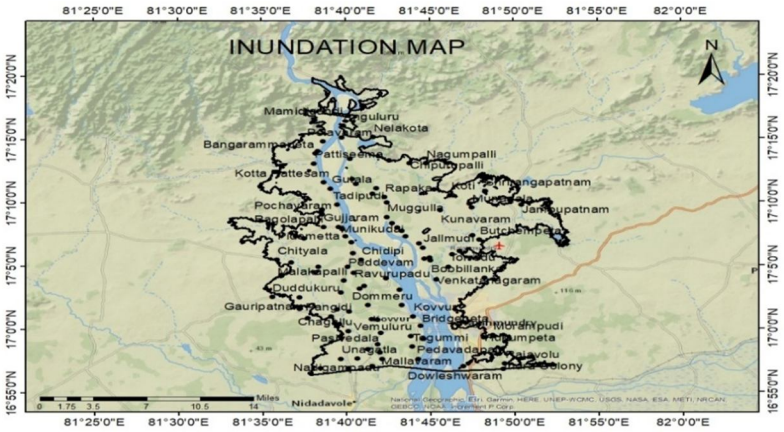

Fig. 10 Villages and towns located within the flood inundation boundary (Black line) of the Polavaram Dam, shown on a satellite base image.

VIII. CONCLUSIONS

This study carried out a two-dimensional dam break analysis and flood inundation mapping of the Polavaram Dam using HEC-RAS 6.6. Breach of the ECRF dam section was simulated for overtopping and piping failure using five empirical breach methods, and the resulting flood was mapped over the downstream floodplain. The main conclusions are as follows.

1) *The breach method has a strong influence:* the peak breach discharge ranged from 32,434 m³/s to 174,862 m³/s, a difference of more than five times, and the inundation area ranged from 172.863 km² to 717.224 km² among the ten scenarios.
2) *The most severe scenario:* the Froehlich (2008) overtopping scenario gave the largest breach width (753.04 m), the highest peak discharge (174,862 m³/s) and the largest inundation area (717.224 km²). The corresponding piping scenario gave 120,453 m³/s and 559.097 km².
3) *Overtopping versus piping:* for every method, overtopping produced a larger inundation area than piping.
4) *Downstream locations:* Area 1 experienced the highest flood-wave velocities (1.865 to 3.937 m/s). The maximum flood depths were 17.138 m at Area 1, 10.682 m at Area 2 and 15.772 m at Area 3, and overtopping generally produced higher depths and water surface elevations than piping.
5) *Use of the results:* the inundation maps and the depth, velocity and water surface elevation values can support dam safety assessment, emergency action planning, evacuation planning and flood-hazard assessment downstream of the Polavaram Dam, and can serve as a basis for detailed flood-risk, vulnerability and damage assessment.

IX. ACKNOWLEDGMENT

The authors gratefully acknowledge the Polavaram Irrigation Project Head Works Circle (PIPHW), Dowalaiswaram, East Godavari district, Andhra Pradesh, for providing the necessary data related to the Polavaram Dam, and the Department of Civil Engineering, University College of Engineering Kakinada (A), JNTUK Kakinada, for institutional support during this study.

REFERENCES

[1] D. C. Froehlich, “Embankment dam breach parameters revisited,” in *Proc. 1995* ASCE Conf. Water Resources Engineering, 1995, pp. 887–891.
[2] D. C. Froehlich, “Embankment dam breach parameters and their uncertainties,” J. Hydraul. Eng., vol. 134, no. 12, pp. 1708–1721, 2008.
[3] T. C. MacDonald and J. Langridge-Monopolis, “Breaching characteristics of dam failures,” J. Hydraul. Eng., vol. 110, no. 5, pp. 567–586, 1984.
[4] J. L. Von Thun and D. R. Gillette, Guidance on Breach Parameters, U.S. Dept. of the Interior, Bureau of Reclamation, Denver, CO, USA, 1990.
[5] Y. Xu and L. M. Zhang, “Breaching parameters for earth and rockfill dams,” J. Geotech. Geoenviron. Eng., vol. 135, no. 12, pp. 1957–1970, 2009.
[6] J. E. Costa, Floods from Dam Failures, U.S. Geological Survey Open-File Report 85-560, Denver, CO, USA, 1985.
[7] Y. Xiong, “A dam break analysis using HEC-RAS,” J. Water Resour. Protect., vol. 3, pp. 370–379, 2011.
[8] I. R. Karim, Z. F. Hassan, H. H. Abdullah, and I. A. Alwan, “2D-HEC-RAS modeling of flood wave propagation in a semi-arid area due to dam overtopping failure,” Civil Eng. J., vol. 7, no. 9, pp. 1501–1514, 2021.
[9] S. A. Hosseinzadeh-Tabrizi, M. Ghaeini-Hessaroeyeh, and M. Ziaadini-Dashtekhaki, “Numerical simulation of dam-breach flood waves,” Appl. Water Sci., vol. 12, no. 5, Art. no. 97, 2022.
[10] C. Mo, Y. Shen, X. Lei, H. Ban, Y. Ruan, S. Lai, W. Cen, and Z. Xing, “Simulation of one-dimensional dam-break flood routing based on HEC-RAS,” Front. Earth Sci., vol. 10, Art. no. 1027788, 2023.
[11] Y. Paşa, İ. B. Peker, A. Hacı, and S. Gülbaz, “Dam failure analysis and flood disaster simulation under various scenarios,” Water Sci. Technol., vol. 87, no. 5, pp. 1214–1231, 2023.
[12] M. J. Mohamed, I. R. Karim, M. Y. Fattah, and N. Al-Ansari, “Modelling flood wave propagation as a result of dam piping failure using 2D-HEC-RAS,” Civil Eng. J., vol. 9, no. 10, pp. 2503–2515, 2023.
[13] T. A. Basheer, A. Wayayok, B. Yusuf, and M. R. Kamal, “Dam breach parameters and their influence on flood hydrographs for Mosul Dam,” J. Eng. Sci. Technol., vol. 12, no. 11, pp. 2896–2908, 2017.
[14] M. Bhandari, N. Nyaupane, S. R. Mote, A. Kalra, and S. Ahmad, “2D unsteady flow routing and flood inundation mapping for lower region of Brazos River watershed,” in Proc. World Environmental and Water Resources Congress *2017*, Sacramento, CA, USA, 2017, pp. 292–303.
[15] O. S. Balogun and H. O. Ganiyu, “Study and analysis of Asa River hypothetical dam break using HEC-RAS,” *Niger. J. Technol.*, vol. 36, no. 1, pp. 315–321, 2017.

©IJRASET: All Rights are Reserved

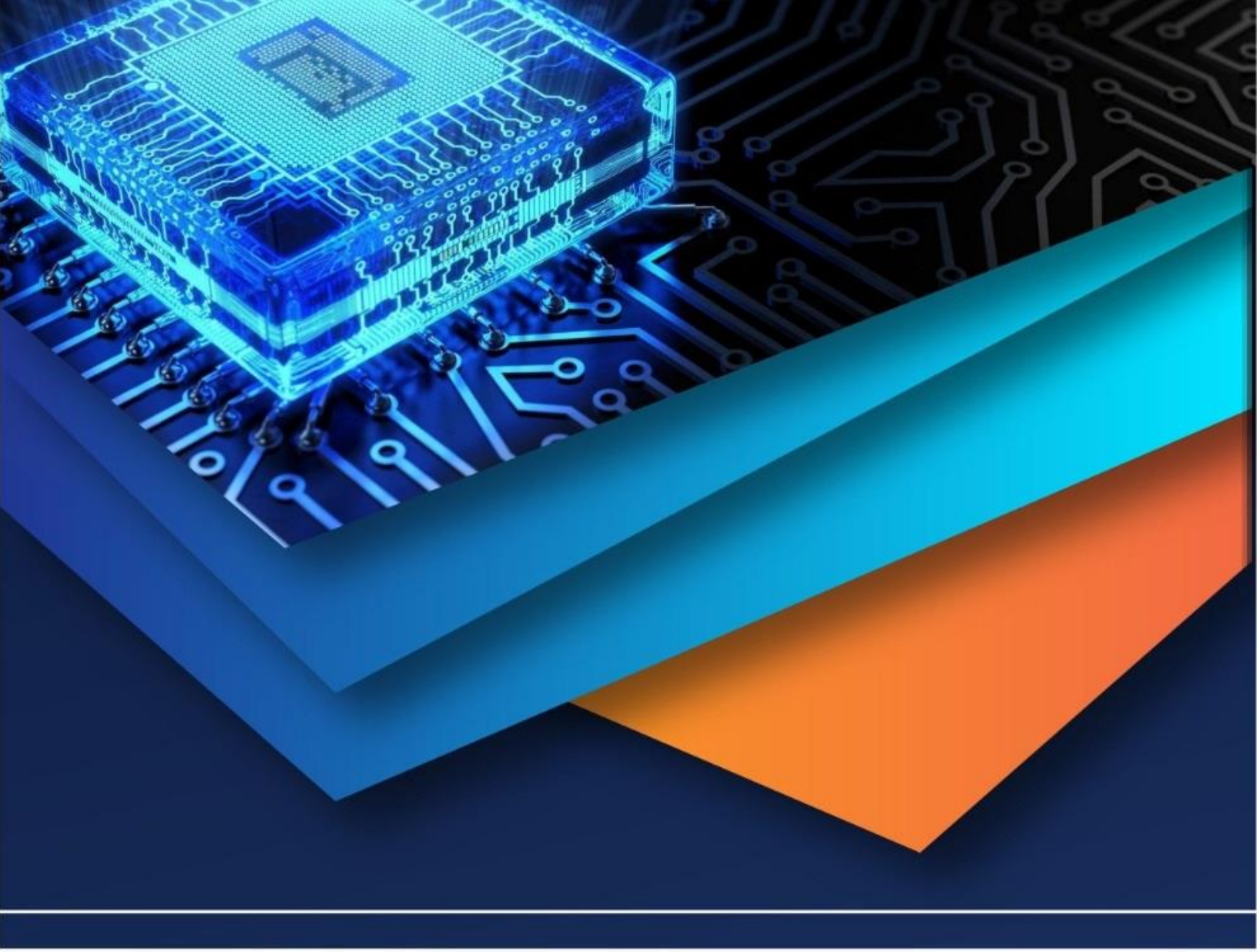

10.22214/IJRASET

45.98

IMPACT FACTOR: 7.129

IMPACT FACTOR: 7.429

INTERNATIONAL JOURNAL FOR RESEARCH

IN APPLIED SCIENCE & ENGINEERING TECHNOLOGY

Call : 08813907089 (24*7 Support on Whatsapp)